UC Irvine
UC Irvine Previously Published Works

Title
Closed form formulas and tunability of resonances in pairs of gold-dielectric nanoshells

Permalink
https://escholarship.org/uc/item/0vr8k83j

ISBN
9780819482532

Authors
Campione, Salvatore
Vallecchi, Andrea
Capolino, Filippo

Publication Date
2010-08-19

DOI
10.1117/12.864036

Copyright Information

Peer reviewed

Closed form formulas and tunability of resonances in pairs of gold-dielectric nanoshells

Salvatore Campione[a], Andrea Vallecchi[a,b], Filippo Capolino*[a]

[a]Dept. of Electrical Engineering and Computer Science, University of California, Irvine, CA, USA 92697

[b]Dept. of Information Engineering, University of Siena, 53100 Siena, Italy

ABSTRACT

Analyses of the resonances of both symmetric and antisymmetric polarization states in pairs of tightly coupled nanoshells, made of either a gold-core/dielectric-shell or a dielectric-core/gold-shell, are carried out at optical frequencies. The nanoparticles are modeled as single electric dipoles, at first considering only the static (non retarded) field terms and resorting to closed-form expressions to investigate the transverse and longitudinal (with respect to the pair axis) plasmonic resonance frequencies of the nanoshell pair. These approximate resonance values are then compared to the ones obtained including all dynamical retarded field terms, and with full wave simulations. We also show how the additional degree of freedom provided by using nanoshells, in contrast to using solid metallic nanoparticles, can be exploited for tuning the symmetric and antisymmetric resonance frequencies in pairs of tightly coupled nanoshells. Indeed, optical resonances of nanoshells can be varied over hundreds of nanometers in wavelength, across the visible and into the infrared region of the spectrum, by varying the relative dimensions of the core and shell. This makes the pair suitable as a constituent for metamaterials since it supports an antisymmetric mode that can be interpreted as an effective magnetic dipole; therefore, it is useful for providing artificial magnetism in metamaterials that may support backward propagation or have equivalent high/low characteristic wave impedance. Furthermore, we show the field enhancement between the two nanoparticles which may find applications in surface enhanced Raman scattering. We also show how an incident field excites the transversal and longitudinal modes supported by the pair.

Keywords: nanoshells, plasmonics, metamaterials, scattering.

1. INTRODUCTION AND STATEMENT OF THE PROBLEM

Subwavelength-size metal nanoparticles can be employed in a wide range of different applications, such as surface-enhanced Raman scattering (SERS), near-field enhancement and subwavelength imaging, due to their ability of providing strong enhancement of the scattered field. This strong enhancement can be explained by the generation of localized surface plasmon resonances, which are due to the coupling between the photons of the incident light at certain frequencies and resonant collective oscillations of free electrons at the metal surface.

The plasmonic properties of a nanostructure depend dramatically on its size and shape. Plasmonic pairs of nanoparticles have been studied deeply and have been used to create artificial magnetism. Plasmon theory applied to nanoparticle pairs has led to the understanding of pair plasmon modes as symmetric and antisymmetric hybridized modes of the characteristic plasmons of the constituent nanoparticles.

A particularly useful nanoparticle is the metal-dielectric nanoshell. By varying the relative dimensions of the core and shell, the optical resonance of such a nanoparticle can be varied over a wide spectral region across the visible and into the infrared. Indeed, the purpose of this paper is to characterize the resonant behavior of a gold-dielectric nanoshell pair by varying the structure parameters, stressing resonances' tunability.

*f.capolino@uci.edu; phone 1 949-824-2164; http://capolino.eng.uci.edu/

The system analyzed in this paper is composed by a pair of electromagnetically coupled nanoshells, and is presented in Fig. 1. In detail, Fig. 1(a) shows a gold core-dielectric shell nanosphere, whereas Fig. 1(b) shows a dielectric core-gold shell nanosphere. The structure is characterized by a core with radius r_1 and permittivity ε_1, a shell with radius r_2 and permittivity ε_2, and the center-to-center distance d between the two nanoparticles. The reference system shown in Fig. 1 will be adopted throughout the paper.
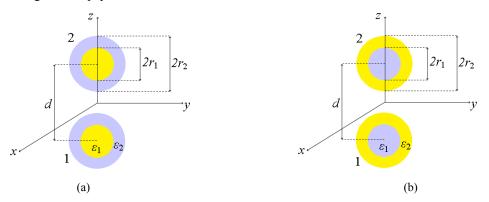

Fig. 1. Geometry of a pair of tightly coupled gold nanoshells. (a) Gold core and dielectric shell. (b) Dielectric core and gold shell.

In this paper we briefly summarize the analytical results obtained in [1]. There, the numerical results were relevant to the case of silver-dielectric nanoshells. In this paper instead we consider the case of gold-dielectric nanoshells. Gold losses are slightly larger than those of silver, and the gold plasma frequency is slightly smaller than the silver one, resulting in a different combination of symmetric and antisymmetric resonances when excited by a single plane wave.

In this paper, we show how the additional degree of freedom provided by using gold-dielectric nanoshells, in contrast to using solid gold nanoparticles, impacts on the tuning of both symmetric and antisymmetric resonance frequencies in pairs of electromagnetically coupled gold nanoparticles.

The structure of the paper is as follows. In Sec. 2, we briefly summarize the theoretical background of the analysis, based on the developments presented in [1]. In particular, the nanoparticles are modeled by using the single dipole approximation (SDA) [2]. We also recall the derivation of the closed-form formulas representing the four resonance frequencies in a pair of nanoshells [1], performed by combining the SDA with a quasistatic approximation for the field emitted by the dipole, valid for small and very close nanoshells. In Sec. 3, we provide some numerical results to show resonance tunability, and the excitation of the resonant modes identified by the SDA by an illuminating wave field is discussed presenting some full-wave simulation results.

2. FORMULATION

In this section, we briefly summarize the concepts that lead to the closed-form expressions for both the transverse and longitudinal resonances of a pair of tightly coupled nanoshells obtained in [1].

2.1 Description of the mathematical procedure

As stated in Sec. 1, we assume that each nanoparticle can be represented as an electric dipole, by using the single dipole approximation (SDA) approach. In this analysis, electromagnetic fields are assumed to be time harmonic with an $e^{-i\omega t}$ time variation.

The electric field at the position r_2 (at the center of the nanoshell #2 in Fig. 1) generated by a dipole with dipole moment p_1 placed at the position r_1 (at the center of the nanoshell #1 in Fig. 1) can be expressed by means of the dyadic Green's function $E(r_2) = \underline{G}(r_2, r_1) \cdot p_1$ (for the expressions and properties of the used dyadic Green's function $\underline{G}(r_2, r_1)$ the reader is referred to [1]). The induced dipole moment p of a subwavelength nanoshell immersed in an electric field is given by $p = \varepsilon_0 \varepsilon_h \alpha E$, where E is the local electric field at the particle location, α is the electric

polarizability of the nanoparticle, ε_0 is the vacuum permittivity, and ε_h is the relative permittivity of the host medium. As shown in [1], the quasi-static approximation for the inverse electric polarizability of a nanoshell is [3-5]

$$\frac{1}{\alpha} = \frac{1}{4\pi r_2^3} \frac{(\varepsilon_2 + 2\varepsilon_h)(\varepsilon_1 + 2\varepsilon_2) + 2\beta(\varepsilon_2 - \varepsilon_h)(\varepsilon_1 - \varepsilon_2)}{(\varepsilon_2 - \varepsilon_h)(\varepsilon_1 + 2\varepsilon_2) + \beta(2\varepsilon_2 + \varepsilon_h)(\varepsilon_1 - \varepsilon_2)} - i\frac{k_h^3}{6\pi}, \tag{1}$$

where ε_h is the relative permittivity of the host medium, ε_1 is the relative permittivity of the core (of radius r_1), and ε_2 is the relative permittivity of the shell (of external radius r_2). Furthermore, $\beta = \rho^3$, with $\rho = r_1/r_2$ and $k_h = \omega\sqrt{\varepsilon_h}/c = k_0\sqrt{\varepsilon_h}$ is the host wavenumber, where k_0 denotes the free space wavenumber. The last imaginary term in (1) has been introduced to account for particle radiation [2-3].

The permittivity dependence of the metal versus frequency is described by the Drude model

$$\varepsilon_m = \varepsilon_\infty - \frac{\omega_p^2}{\omega(\omega + i\gamma)}, \tag{2}$$

where ω_p is the plasma angular frequency, γ is the damping term, and ε_∞ is a "high frequency" permittivity. All these parameters can be determined to match experimental data.

Our purpose is to find the resonance frequencies (eigenvalues) and polarization states (eigenvectors) of the two nanoshell system (Fig. 1) by solving the two coupled equations described in [1], obtaining two scalar equations, one for the transverse polarization (electric dipole moment orthogonal to the axis of the pair, z) and one for the longitudinal polarization (electric dipole moment along the axis of the pair).

We repeat here for the sake of completeness the scalar equations that need to be solved to get the resonance frequencies of the pair [1]. In particular, the resonances for the two *transverse* antisymmetric/symmetric polarizations are found by solving numerically

$$\left(c_1 \pm \frac{1}{\varepsilon_0\varepsilon_h\alpha}\right) = 0, \qquad c_1 = \frac{e^{ik_hd}}{4\pi\varepsilon_h\varepsilon_0}\left(\frac{k_h^2}{d} + \frac{ik_h}{d^2} - \frac{1}{d^3}\right), \tag{3}$$

where the "$+$" sign is for the antisymmetric mode ($p_2 = -p_1$), whereas the "$-$" sign is for the symmetric one ($p_2 = p_1$). Analogously, the resonances for the *longitudinal* antisymmetric/symmetric polarizations are found from

$$\left(c_3 \pm \frac{1}{\varepsilon_0\varepsilon_h\alpha}\right) = 0, \qquad c_3 = -\frac{e^{ik_hd}}{4\pi\varepsilon_h\varepsilon_0}\left(\frac{2ik_h}{d^2} - \frac{2}{d^3}\right). \tag{4}$$

The eigenvectors p_1 and p_2 associated to the four resonances are shown in Fig. 2. The two resonance frequencies f_{t1} and f_{t2} associated to the two *transverse* (with respect to the pair axis) resonances in Figs. 2(b) and 2(c) are solutions of equation (3), with the "$+$" (antisymmetric) and "$-$" (symmetric) sign, respectively. The two eigenfrequencies $f_{\ell1}$ and $f_{\ell2}$ associated to the two *longitudinal* (parallel to the pair axis) resonances in Figs. 2(d) and 2(a) are solutions of equation (4), with the "$+$" (antisymmetric) and "$-$" (symmetric) sign, respectively.
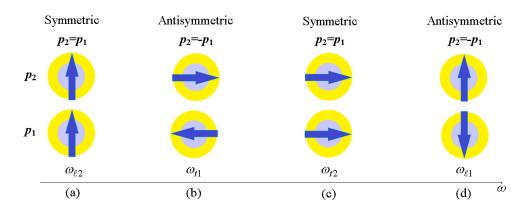
Fig. 2. Four possible resonance states in a pair of nanoshells. Both transverse (t) and longitudinal (ℓ) resonance modes exhibit symmetric and antisymmetric configurations. The resonance order is the limiting case valid under the quasistatic (QS) approximation.

2.2 Quasi-static approximation for deriving closed-form formulas

In this paper, we report analytical expressions for the resonances associated to a nanoshell pair that were previously derived in [1]. In deriving the final expressions some electrodynamic terms have been replaced by their electrostatic approximations because the particles are small compared to the free space wavelength. In SDA calculations this is equivalent to setting $k_h = 0$ but keeping the correct frequency-dependent dielectric constant ε_m in (2) (see [1] for more details). This approximation applies specifically to the dynamics of a single particle, but it is here used in combination with the SDA method to describe the electromagnetic behaviour of a pair of nanoshells. Therefore, after neglecting the dynamic terms (in other words we keep only the $1/d^3$ terms in (3) and (4)) and by taking into account that $\gamma << \omega_p$, (3) and (4) are solved analytically for the resonant angular frequencies leading to the expressions for transverse and longitudinal polarizations for the two cases of gold core-dielectric shell and dielectric core-gold shell.

2.2.1 Quasi-static approximation for gold core – dielectric shell nanospheres

For the *transverse* polarization, the procedure described above leads to

$$\omega_{t1,2} = \frac{\omega_p}{\sqrt{\varepsilon_\infty + \varepsilon_2 \dfrac{b' - b''(\pm\delta)}{a' - a''(\pm\delta)}}} - i\frac{\gamma}{2}, \tag{5}$$

whereas for *longitudinal* polarization the expression is

$$\omega_{\ell 1,2} = \frac{\omega_p}{\sqrt{\varepsilon_\infty + \varepsilon_2 \dfrac{b' - b''(\mp 2\delta)}{a' - a''(\mp 2\delta)}}} - i\frac{\gamma}{2}. \tag{6}$$

Here, $\delta = (r_2/d)^3$, and the upper/lower sign applies to the antisymmetric/symmetric polarization. The formula coefficients are

$$a' = 2\beta(\varepsilon_2 - \varepsilon_h) + (\varepsilon_2 + 2\varepsilon_h), \quad a'' = \beta(2\varepsilon_2 + \varepsilon_h) + (\varepsilon_2 - \varepsilon_h), \tag{7}$$

$$b' = -2\beta(\varepsilon_2 - \varepsilon_h) + 2(\varepsilon_2 + 2\varepsilon_h), \quad b'' = -\beta(2\varepsilon_2 + \varepsilon_h) + 2(\varepsilon_2 - \varepsilon_h). \tag{8}$$

Note that expression (6) is the same as (5) after replacing δ by -2δ. For $\varepsilon_h = 1$ (nanoshells in vacuum), and $\varepsilon_1 = \varepsilon_2$ (core and shell made of the same material) these expressions coincide with those in [6] and [7].

2.2.2 Quasi-static approximation for dielectric core – gold shell nanospheres

The procedure previously described leads to the following closed-form expression for the transverse antisymmetric (upper sign) and symmetric (lower sign) modes

$$\omega_{t1,2} = \frac{\omega_p}{\sqrt{2}} \sqrt{\frac{a'(\pm\delta) + a'' - \sqrt{\left[b'(\pm\delta) + c''\right]^2 - 36\varepsilon_1\varepsilon_h\beta(\delta^2 \pm \delta - 2)}}{(d' + b''\varepsilon_\infty)(\pm\delta) - d'' + c'\varepsilon_\infty}} - i\frac{\gamma}{2}, \tag{9}$$

whereas, for the longitudinal antisymmetric (upper sign) and symmetric (lower sign) modes, we have

$$\omega_{\ell1,2} = \frac{\omega_p}{\sqrt{2}} \sqrt{\frac{a'(\mp 2\delta) + a'' - \sqrt{\left[b'(\mp 2\delta) + c''\right]^2 - 36\varepsilon_1\varepsilon_h\beta(4\delta^2 \mp 2\delta - 2)}}{(d' + b''\varepsilon_\infty)(\mp 2\delta) - d'' + c'\varepsilon_\infty}} - i\frac{\gamma}{2}, \tag{10}$$

with

$$a' = \varepsilon_h(\beta + 2) - \varepsilon_1(2\beta + 1) + 4\varepsilon_\infty(\beta - 1), \quad a'' = 2\varepsilon_h(\beta + 2) + \varepsilon_1(2\beta + 1) - 4\varepsilon_\infty(\beta - 1), \tag{11}$$

$$b'^{,''} = \varepsilon_h(\beta + 2) \pm \varepsilon_1(2\beta + 1), \quad c'^{,''} = 2\varepsilon_h(\beta + 2) \pm \varepsilon_1(2\beta + 1), \tag{12}$$

$$d' = (\beta - 1)(2\varepsilon_\infty^2 - \varepsilon_1\varepsilon_h), \quad d'' = 2(\beta - 1)(\varepsilon_\infty^2 + \varepsilon_1\varepsilon_h). \tag{13}$$

As in the previous case, note that (10) is the same as (9) after replacing δ by -2δ.

3. ANALYSES OF NUMERICAL AND FULL-WAVE SIMULATION RESULTS

In this section, we analyze the properties of the pair of nanoshells in the particular case in which the dielectric material is *glass* (whose permittivity is equal to $\varepsilon = 2.25$) and the metal is *gold*, embedded in an environment with $\varepsilon_h = 1$, though the reported expressions are valid for arbitrary host permittivities. We recall that in [1] we used glass as dielectric and silver as a metal, in all the implemented analyses. Therefore in this paper we analyze the same structures and properties analyzed in [1] for the case of gold-dielectric nanoshells. The adopted Drude model parameters to characterize the permittivity of gold with respect to frequency are taken from [8]: $\omega_p = 1.36 \times 10^{16} \, rad/s$, $\gamma = 1.05 \times 10^{14} \, s^{-1}$, and $\varepsilon_\infty = 9.5$. We chose these parameters because they agree well with the experimental results presented in [9] by Johnson and Christy in the frequency range of interest for this paper, that is 400−650 THz.

3.1 Resonance of a single nanoshell

An inspection of the resonance frequency of a single nanoshell is provided in this section for comparison with resonance frequencies of the pair of nanoshells. Real and imaginary parts of this resonance (f_r) are shown in Fig. 3(a) for a gold core-dielectric shell nanosphere and in Fig. 3(b) for a dielectric core-gold shell nanosphere.

As can be easily noticed, the resonance frequency of the single nanoparticle falls in the frequency range (400−650 THz) in which the adopted Drude model for the gold is correctly approximating the experimental results in [9]. Furthermore, note the wide tunable range of the resonance frequency in case of dielectric core-gold shell nanosphere by varying the radii ratio $\rho = r_1/r_2$.
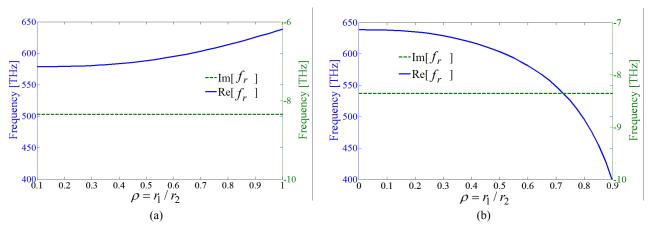
Fig. 3. Real and imaginary parts of the resonance frequency versus ratio of radii for a single nanoshell ($r_2 = 50$ nm) for (a) the gold core-dielectric shell and (b) the dielectric core-gold shell structure.

3.2 Resonances tunability of the nanoshell pair

In this section, we present some numerical results to show the tunability of the resonance frequencies by varying the core radius r_1, the shell radius r_2 and the center-to-center distance d.

The results computed by the closed-form expressions (5)−(6) and (9)−(10) derived by retaining only the quasistatic (denoted as "QS", dashed curves in Figs. 4−9) dipolar field terms are compared with those obtained by including in the calculations all the dynamic field components of the dipole radiation (3) and (4), which are denoted as "Dyn" (straight curves in Figs. 4−9).

The imaginary part of the frequency solutions represents the total amount of material and radiation losses. As can be observed from Figs. 4−9, the resonances of the symmetric modes in Figs. 2(c) and 2(a), f_{t2} and $f_{\ell2}$, have a larger imaginary part than f_{t1} and $f_{\ell1}$, the resonances of the antisymmetric modes in Figs. 2(b) and 2(d). This is due to the fact that radiation losses for symmetric modes are significantly larger since the pair of nanoshells radiates like a dipole, whereas the two radiation contributions associated to the two antisymmetric (opposite) dipoles tend to cancel out. In other words, the transverse resonance for the antisymmetric pair tends to radiate like a magnetic dipole [6, 10] plus an electric quadrupole [10]. Indeed, the antisymmetric mode is associated to a current loop (magnetic dipole) and it is a classic result of antenna theory that a small loop radiates less than a small dipole of same current and dimension. Note that the *transverse* antisymmetric resonance frequency f_{t1} is smaller than the symmetric one f_{t2}, for all cases considered. Also, note that the *longitudinal* symmetric resonance frequency $f_{\ell2}$ is smaller than the antisymmetric one $f_{\ell1}$, except for very small values of $\tau = r_2/d$. And in general (but not always), the resonances are ordered as $f_{\ell2} < f_{t1} < f_{t2} < f_{\ell1}$. It is also noted that at small ratios $\tau = r_2/d$ the real parts of the four resonance frequencies tend to be similar, and close to the resonance of a single particle, due to weaker coupling.

It is noteworthy that in all the analyzed cases, the prediction of the imaginary part of the resonant frequencies employing only the quasistatic dipole terms is very poor. This is because the dipole radiation terms $1/d$ are not accounted for in the QS estimate. For the symmetric resonances, where radiation is stronger, the QS prediction is indeed poorer. We recall that, as shown in [2] and [11], the SDA starts to fail when the center-to-center distance d of the two nanoshells is smaller than $3r_2$.

3.2.1 Core radius r_1 parameterization

The real and imaginary parts of the four resonance frequencies of a pair of nanoshells are plotted versus the ratio of the core and shell radii $\rho = r_1/r_2$ in Fig. 4 for the gold core-dielectric shell case, and in Fig. 5 for the dielectric core-gold shell one, keeping the nanoshells center-to-center distance at $d = 125$ nm and the shell radius at $r_2 = 50$ nm.
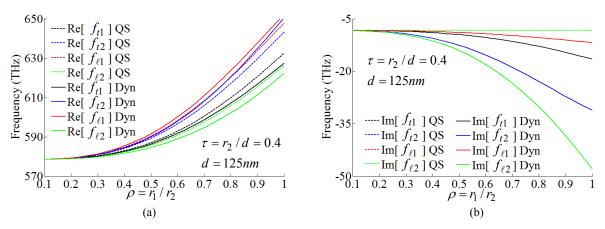
Fig. 4. Real and imaginary parts of the four resonance frequencies versus ratio of radii, for a sphere distance $d = 125$ nm ($r_2 = 50$ nm) for the gold core-dielectric shell structure. "Dyn" means that all dipolar dynamic field components are considered; "QS" means that only the static component $1/d^3$ of the dipolar field is considered.
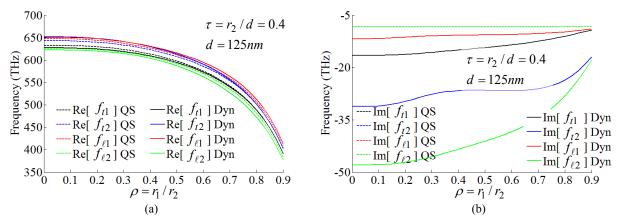

Fig. 5. Real and imaginary parts of the four resonance frequencies versus ratio of radii, for a sphere distance $d = 125$ nm ($r_2 = 50$ nm) for the dielectric core-gold shell structure.

It can be observed from Figs. 4 and 5 that the dynamic and quasistatic solutions agree well for small values of the ratio of radii (with fixed $d = 125$ nm) for the case in Fig. 1(a), and for high values of the ratio of radii (with fixed $d = 125$ nm) for the case in Fig. 1(b). In general, the QS approximation is less accurate than the fully dynamic solution; this is due to the fact that QS considers only the $1/d^3$ field term, and neglects the effect of retardation in the coupling mechanism between the two nanoshells and the $1/d$ and $1/d^2$ field terms. Thus, QS results become less accurate when the coupling between the two nanoshells becomes stronger.

3.2.2 Shell radius r_2 parameterization

The real and imaginary parts of the four resonance frequencies are plotted versus the ratio $\tau = r_2/d$ of the shell radius to the center-to-center distance in Fig. 6 for the gold core-dielectric shell case, and in Fig. 7 for the dielectric core-gold shell one, with fixed $d = 75$ nm and $\rho = r_1/r_2 = 0.8$ (i.e., the nanoshell radius r_2 is variable here).

To illustrate that the stronger the coupling between the two nanoshells is, the less accurate QS results are, in Figs. 6 and 7 we show that for larger shell radius r_2 (and therefore for larger scattered field) the QS approximation tends to diverge from the dynamic solution because it cannot correctly describe the interaction between the particles (both are based on the SDA).
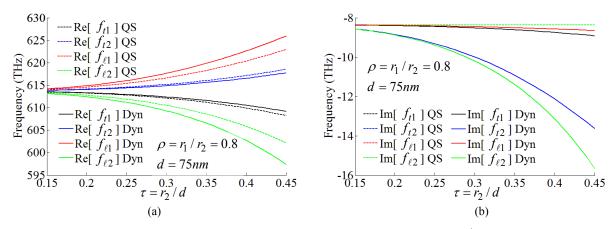
Fig. 6. Real and imaginary parts of the four resonance frequencies versus the ratio $\tau = r_2/d$ for fixed distance $d = 75$ nm between the nanoshells (i.e., the shell radius r_2 is variable) and $\rho = r_1/r_2 = 0.8$ for the gold core-dielectric shell structure.
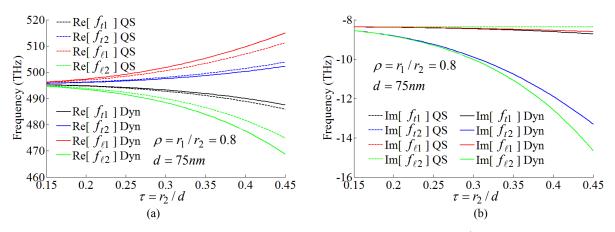

Fig. 7. Real and imaginary parts of the four resonance frequencies versus the ratio $\tau = r_2/d$ for fixed distance $d = 75$ nm between the nanoshells (i.e., the shell radius r_2 is variable) and $\rho = r_1/r_2 = 0.8$ for the dielectric core-gold shell structure.

3.2.3 Center-to-center distance *d* parameterization

The real and imaginary parts of the four resonance frequencies are plotted versus the ratio $\tau = r_2/d$ in Fig. 8 for the gold core-dielectric shell case, and in Fig. 9 for the dielectric core-gold shell one, with fixed shell radius $r_2 = 40$ nm and $\rho = r_1/r_2 = 0.8$ (i.e., the center-to-center distance d between the nanoshells is variable here).
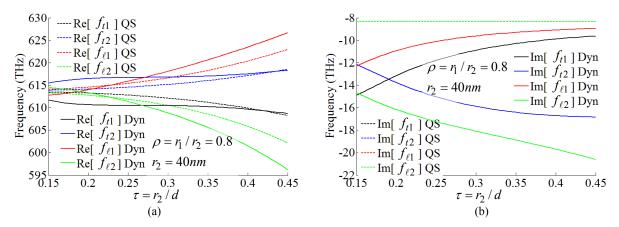
Fig. 8. Real and imaginary parts of the four resonance frequencies versus the ratio $\tau = r_2/d$ for fixed shell radius $r_2 = 40$ nm (i.e., the distance d between the nanoshells is variable) and $\rho = r_1/r_2 = 0.8$ for the gold core-dielectric shell structure.
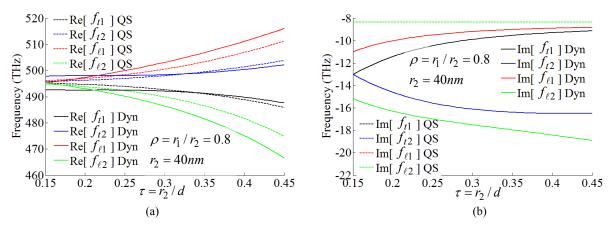

Fig. 9. Real and imaginary parts of the four resonance frequencies versus the ratio $\tau = r_2/d$ for fixed shell radius $r_2 = 40$ nm (i.e., the nanoshell distance d is variable) and $\rho = r_1/r_2 = 0.8$ for the dielectric core-gold shell structure.

In Figs. 8 and 9, the "QS" and "Dyn" solutions, though in general agreement with each other, show a small difference which is more or less independent from the distance d. This is because though the QS approximation for small d is expected to be better than for large d, the amount of coupling between the nanoshells is inversely proportional to d, and the influence of the coupling on the estimation of the resonant frequencies affects the overall approximation.

3.3 Full-wave analysis (dielectric core - gold shell)

The above concepts are here tested for the case of a dielectric core - gold shell pair by comparing results obtained by the SDA with those by the full-wave electromagnetic solver CST Microwave Studio.

3.3.1 Excitation of transverse resonances

We observe the excitation of the antisymmetric and symmetric modes. Considering the geometry in Fig. 1, these can be excited by using two types of excitation: (i) either a pair of antisymmetric or symmetric (with respect to the electric field) plane waves, arriving from the $+z$ and $-z$ directions, or (ii) a single plane wave coming from $+z$. The incoming electric field is polarized along y for all considered excitations.

Figure 10(a) shows the magnitude of the y-component of the electric field at the center of the nanoshell at $\mathbf{r}_2 = \hat{z}d/2$, excited by the plane wave pair, whereas Fig. 10(b) shows the magnitude of the y-component of the electric field at the

center of both nanoshells, at $r_1 = -\hat{z}d/2$ and $r_2 = \hat{z}d/2$, excited by single plane wave, for the dielectric core-gold shell structure. In other words, an incident plane wave E_{inc}, polarized along y, can be represented (Fig. 10(a)) as $E_{inc} = E_{sym} + E_{antisym}$, where E_{sym} is made by a pair of plane waves arriving from the $+z$ and $-z$ directions, with E field y-components in phase at $z = 0$ (also called perfect magnetic conductor (PMC) symmetry), and $E_{antisym}$ is made by a pair of plane waves arriving from the $+z$ and $-z$ directions, with E field y-components out of phase at $z = 0$ (also called perfect electric conductor (PEC) symmetry). It is clear that E_{sym} excites only the symmetric resonance in Fig. 2(c), whereas $E_{antisym}$ excites the antisymmetric one in Fig. 2(b).

When using the SDA, the field E_i at a center of a nanoshell i=1,2 is found by using the expression [1]

$$p_i = \frac{4}{9}\pi r_2^3 \frac{\varepsilon_0}{\varepsilon_2}\left[(\varepsilon_2 - \varepsilon_h)(\varepsilon_1 + 2\varepsilon_2) + \beta(2\varepsilon_2 + \varepsilon_h)(\varepsilon_1 - \varepsilon_2)\right]E_i, \qquad (14)$$

once the nanoshell equivalent dipole polarization p_i has been determined by using the SDA method outlined in [11].

The first structure under analysis has the shell outer radius r_2=35 nm, the ratio of the radii $\rho = r_1/r_2 = 0.8$ and the center-to-center distance d =100 nm.

The antisymmetric excitation has a null of the electric field at the symmetry plane $z = 0$ and excites only the antisymmetric mode that has a magnitude peak, which corresponds to the transverse antisymmetric resonance f_{t1}, at f = 493 THz when using the SDA and at f = 482 THz when using CST. The blue shift of the SDA compared to the CST full wave results is in agreement with previous observations [2]. The symmetric excitation has a maximum of the electric field at $z = 0$ and excites only the symmetric mode that has a peak, denoting the transverse symmetric resonance f_{t2}, at f = 500 THz when using the SDA and at f = 493 THz when using CST. These peak location frequency values (obtained with the SDA and CST) have to be compared with the resonance frequencies obtained by solving equation (3), based on the quasi-static polarizability expression (1), that yields f_{t1} = 492 THz and f_{t2} = 499 THz; they have to be compared as well with the values obtained when using the formula (9), based on the static dipole expressions and the static polarizability expression (1), which yields f_{t1} = 491 THz and f_{t2} = 500 THz. From these comparisons we can conclude that though the SDA, with the static or quasi-static polarizability, fails to predict the exact resonant frequencies, it still provides useful insight in the coupling mechanism of nanoshell pairs. The main reason of the observed frequency shift between SDA and CST results is attributed to the quasi-static polarizability expression (1) we have used. Indeed, when using a more accurate expression for the polarizability based on the Lorenz-Mie theory [3], we expect that the accuracy of SDA could be greatly improved as shown in [2, 12] for the case of metallic nanospheres.

The electric field at the center of each nanoshell induced by a *single* normally incident plane wave polarized along y, is shown in Fig. 10(b), by using the SDA and CST. The superposition of the antisymmetric and symmetric modes field that add up in phase by the upper nanoshell results in a smooth peak of the total field E_2 at its center, whereas the field E_1 at the center of the lower nanoshell exhibits two peaks, corresponding to the antisymmetric and symmetric modes that tend to cancel each other, though the field does not completely vanish at any frequency because of the spectral separation between the two resonances.

The electric and magnetic field distributions induced in a pair of nanoshells by a *single* normally incident plane wave from z and polarized along y, at frequencies f = 482 THz and f = 493 THz, close to the transverse antisymmetric and symmetric resonances, respectively, are illustrated in Fig. 11. There, the arrow plots represent the electric field vector distribution at a certain time instant and are superimposed to the color maps of the magnetic field intensity along x. Consistently with Fig. 10, the field distribution (excited by a *single* plane wave) is not perfectly symmetric or antisymmetric, due to the closeness of the transverse resonances implying that both resonance modes contribute to the total excited field and, as a result, the magnitude of the electric field at the lower nanoshell appears to be smaller than that at the upper one. At any rate, the antisymmetric and symmetric modes tend to prevail by their respective resonant frequencies, as apparent from both the orientation of the electric field and the amplitude of the magnetic field in the gap between the particles that is noticeably enhanced at the antisymmetric resonance frequency.
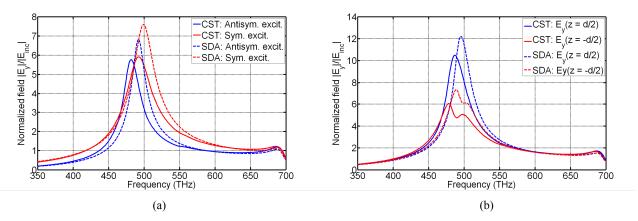
(a)   (b)

Fig. 10. Magnitude of the *y*-component of the electric field at the center of the nanoshells (dielectric core and gold shell with r_2=35 nm, ratio of the radii $\rho = r_1/r_2 = 0.8$ and center-to-center distance d =100 nm), excited by (a) a pair of antisymmetric or symmetric plane waves arriving from the +*z* and –*z* directions, and (b) a single plane wave coming from +*z*, for the dielectric core-gold shell structure.
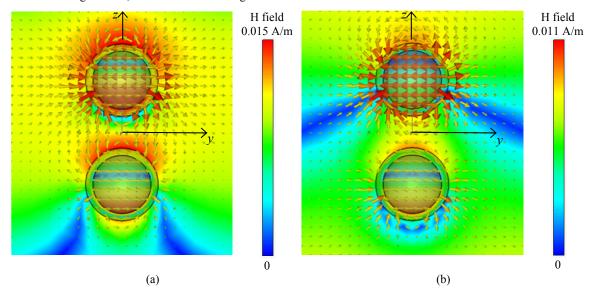

(a)   (b)

Fig. 11. Electric (*y-z* plane) and magnetic (along *x*) field distributions for a pair of gold nanoshells, with shell outer radius r_2=35 nm, ratio of the radii $\rho = r_1/r_2 = 0.8$ and center-to-center distance d =100 nm, for the dielectric core-gold shell structure. (a) Antisymmetric resonance mode excited by a single plane wave coming from +*z* at *f* = 482 THz (note the magnetic field between the two spheres); (b) symmetric resonance mode excited by a single plane wave at *f* = 493 THz. Since the two resonant frequencies, 482 and 493 THz are not well separated, the two distinct modes cannot be separately excited by a single plane wave.

In Fig. 12 we show the same results relative to Figs. 10-11, analyzing a structure with the same parameters except that now the outer shell radius is r_2=50 nm (the ratio of the radii is still $\rho = r_1/r_2 = 0.8$) and the center-to-center distance is d =110 nm. Fig. 12 shows that now the distance between the two resonance frequencies (symmetric and antisymmetric) is larger than the one in the case illustrated in Fig. 10. Therefore it is possible that one incident plane wave is able to excite more strongly the antisymmetric resonance compared to the symmetric one. This is shown in Fig. 13 where the arrows represent the electric field vector distribution at a certain time instant. For this reason, a strong magnetic field is clearly observed near the origin in the field plot in Fig. 13(a) caused by the antisymmetric resonance. The electric field plots are observed in Fig. 13.

These results show that by properly choosing the radii's ratio and distance we can slightly tune the two resonances independently.
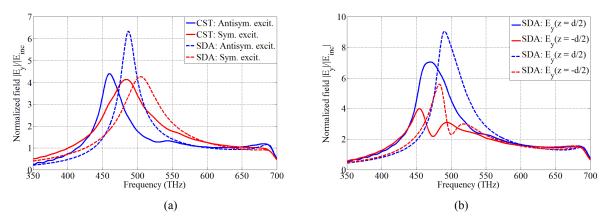
Fig. 12. As in Fig. 10, with the exception that now r_2=50 nm and d =110 nm. The main difference is that now the symmetric and antisymmetric resonances have a distance of 24.7 THz (further apart with respect to the case in Fig. 10).
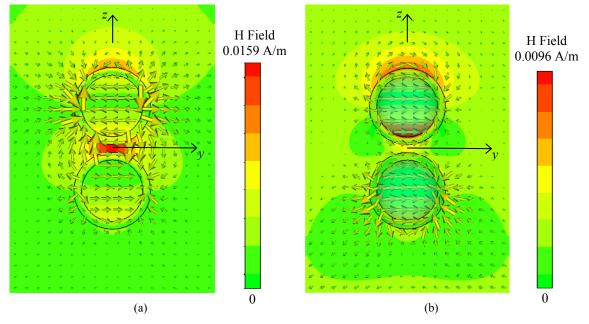

Fig. 13. As in Fig. 11 with the exception that now r_2=50 nm and d =110 nm. The antisymmetric and symmetric resonances (excited by a single plane wave) are shown at frequencies of f = 460 THz and f = 485 THz, respectively. Note that since the resonances are further apart the field at f = 460 THz has a more clear antisymmetric field distribution than that in Fig. 11(a).

3.3.2 Excitation of longitudinal resonances

In this case we show the excitation of the symmetric mode. Considering the geometry in Fig. 1, the nanoshells are excited by using a plane wave arriving from the y direction, with incoming electric field polarized along z. (Note that in this case an antisymmetric excitation made by two plane waves arriving from $-y$ and $+y$ has a null of the electric field at $y = 0$ and would not excite any mode.)

Figure 14 shows the magnitude of the z-component of the electric field at the center of the nanoshells at $\boldsymbol{r}_1 = -\hat{z}d / 2$ and $\boldsymbol{r}_2 = \hat{z}d / 2$ (curves are superimposed because of symmetry) obtained with the SDA and with CST. When using the SDA, the field $\boldsymbol{E}_i$ at a center of a nanoshell i=1,2 is found again by using the expression (14) once the nanoshell

equivalent dipole polarization p_i has been determined. The symmetric mode has a magnitude peak at $f = 483$ THz when using the SDA and at $f = 469$ THz when using CST, which corresponds to the longitudinal symmetric resonance $f_{\ell 2}$ obtained from (4). These frequency peak locations (obtained with the SDA and CST) have to be compared with the resonance frequency obtained by solving equation (4), based on the static polarizability expression (1), that yields $f_{\ell 2} = 482$ THz; they have to be compared as well with the values obtained when using the formula (10), based on the static dipole expressions and the static polarizability expression (1), which yields $f_{\ell 2} = 487$ THz. From these comparisons we can conclude that though the SDA, with the quasi-static polarizability, does not predict the same resonant frequency as CST (cfr. 483 THz with 469 THz), but it still provides useful insight in the coupling mechanism of nanoshell pairs. Indeed, by using a more accurate expression for the polarizability based on the Lorenz-Mie theory [3], we expect that the accuracy of SDA could be greatly improved [2, 12].
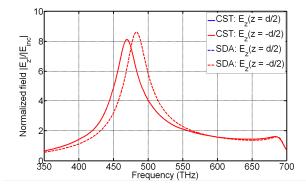

Fig. 14. Magnitude of the *z*-component of the electric field at the center of the shells, excited by a single plane wave arriving from the *y* direction, for the dielectric core-gold shell structure. Shell radius r_2=35 nm, ratio of the radii $\rho = r_1 / r_2 = 0.8$ and center-to-center distance d =100 nm.

In Fig. 15 we show the *z* polarization of the electric field at the center of the pair system, i.e., at the origin, versus frequency, for two slightly different pair configurations. The first one is the same configuration analyzed in previous Fig. 14 with $d = 100$ nm. The second one is a structure with the same parameters except that the center-to-center distance is d =80 nm (i.e. closer nanoshells). The field between the two nanoshells is strongly enhanced and reaches 14 times the value of the incident electric field when $d = 100$ nm and 47 times when d =80 nm.
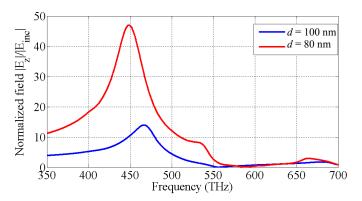

Fig. 15. Magnitude of the *z*-component of the electric field at the center of the pair system, excited by a single plane wave arriving from the *y* direction with electric field polarized along *z*, for the dielectric core-gold shell structure. Shell radius r_2=35 nm, $\rho = r_1 / r_2 = 0.8$, and center-to-center distance $d = 100$ nm and 80 nm. Note the amount of the strongest field enhancement in correspondence of the shortest *d*.

The electric field distribution (in the *y-z* plane) induced in a pair of nanoshells by a *single* incident plane wave from the *y* direction and polarized along *z* at frequency $f = 469$ THz, close to the longitudinal symmetric resonance, is illustrated in Fig. 16. Parameters: r_2=35 nm, $\rho = r_1 / r_2 = 0.8$, and d =100 nm.
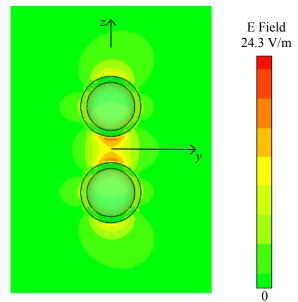
Fig. 16. Electric field distribution (*z*-component in the *y-z* plane) for a pair of gold nanoshells (dielectric core and gold shell with r_2=35 nm, $\rho = r_1/r_2 = 0.8$, and *d* =100 nm) for the symmetric resonance mode excited by a single plane wave at *f* = 469 THz.

4. CONCLUSION

In this paper we have shown the possibility of widely control and tune the resonance frequencies of pairs of tightly coupled nanoshells by varying geometrical parameters, in contrast to using solid metal nanospheres. Based on a quasi-static approximation, we have reported closed-form formulas for predicting resonance frequencies derived in a previous work. We have compared these quasi-static results to the solution including all retarded field terms in the single dipole approximation. Lastly, we have shown with full-wave simulations how transverse and longitudinal resonances can be excited by an illuminating plane wave.

An important aspect of the considered structures is that they have been shown to be able to support an antisymmetric mode that can be interpreted as an effective magnetic dipole; therefore, they could be used to achieve artificial magnetism in metamaterials that may support backward propagation or have equivalent high/low characteristic wave impedance. Moreover, the excitation of the symmetric longitudinal mode strongly enhances the electric field in the center of the paired nanoshells and this configuration can be proposed as a receiving nano-antenna. In a reciprocal way, a small electric dipole placed in the middle of the pair would radiate a strong electric field.

ACKNOWLEDGEMENTS

REFERENCES

[1] A. Vallecchi, S. Campione, and F. Capolino, "Symmetric and antisymmetric resonances in a pair of metal-dielectric nanoshells: tunability and closed-form formulas," *Journal of Nanophotonics,* 4, 041577-13 (2010).
[2] S. Steshenko, and F. Capolino, "Single dipole approximation for modeling collections of nanoscatterers," Chapter 8 in *Theory and Phenomena of Metamaterials*, F. Capolino, Ed., pp. 8.1-8.17, CRC Press, Boca Raton (2009).
[3] C. F. Bohren, and D. R. Huffman, *Absorption and Scattering of Light by Small Particles*, Wiley, New York (1983).
[4] K. Tanabe, "Field enhancement around metal nanoparticles and nanoshells: A systematic investigation," *Journal of Physical Chemistry C,* 112(40), 15721-15728 (2008).
[5] A. Sihvola, *Electromagnetic Mixing Formulas and Applications*, IEEE Publishing, London (1999).

[6] A. Vallecchi, and F. Capolino, "Metamaterials based on pairs of tightly-coupled scatterers," Chapter 19 in *Theory and Phenomena of Metamaterials*, F. Capolino, Ed., pp. 19.1-19.47, CRC Press, Boca Raton (2009).

[7] V. Myroshnychenko, J. Rodriguez-Fernandez, I. Pastoriza-Santos *et al.*, "Modelling the optical response of gold nanoparticles," *Chemical Society Reviews,* 37(9), 1792-1805 (2008).

[8] N. K. Grady, N. J. Halas, and P. Nordlander, "Influence of dielectric function properties on the optical response of plasmon resonant metallic nanoparticles," *Chemical Physics Letters,* 399(1-3), 167-171 (2004).

[9] P. B. Johnson, and R. W. Christy, "Optical Constants of the Noble Metals," *Physical Review B,* 6(12), 4370 (1972).

[10] A. Alu, and N. Engheta, "Dynamical theory of artificial optical magnetism produced by rings of plasmonic nanoparticles," *Physical Review B,* 78(8), (2008).

[11] S. Steshenko, A. Vallecchi, and F. Capolino, "Electric and magnetic resonances in arrays with elements made of tightly coupled silver nanospheres," *Proc. of Metamaterials'.* Pamplona, Spain, 21-26 Sep (2008).

[12] W. T. Doyle, "Optical properties of a suspension of metal spheres," *Physical Review B,* 39(14), 9852-9858 (1989).